Ocean Sci. Discuss., 8, 1441–1466, 2011
www.ocean-sci-discuss.net/8/1441/2011/
doi:10.5194/osd-8-1441-2011

Ocean Science Discussions

Tracer distribution in the Pacific Ocean following a release off Japan – what does an oceanic general circulation model tell us?

H. Dietze and I. Kriest

IFM-GEOMAR, Leibniz Institute of Marine Sciences, Düsternbrooker Weg 20, 24105 Kiel, Germany

Received: 26 May 2011 – Accepted: 6 June 2011 – Published: 21 June 2011

Correspondence to: H. Dietze (hdietze@ifm-geomar.de)

Published by Copernicus Publications on behalf of the European Geosciences Union.

Abstract

In the aftermath of an earthquake and tsunami on 11 March 2011 considerable amounts of radioactive materials were accidentally released into the sea off Fukushima-Daiichi, Japan. This study uses a three-dimensional eddy-resolving oceanic general circulation model to explore potential pathways of a tracer, similar to ^{137}Cs, from the coast to the open ocean. Results indicate that enhanced concentrations meet a receding spring bloom offshore and that the area of enhanced concentrations offshore is strongly determined by surface mixed layer dynamics. However, huge uncertainties remain. Among them are the realism of the simulated cross-shelf transport and apparently inconsistent estimates of the particle reactivity of ^{137}Cs which are discussed in a brief literature review. We argue that a comprehensive set of ^{137}Cs measurements, including sites offshore, could be a unique opportunity to both evaluate and advance the evaluation of oceanic general circulation models.

1 Introduction

Triggered by the recent direct release of radioactive substances from the land to the ocean at Fukushima-Daiichi, Japan, there is a rising interest in how and on what timescales coastal waters are diluted onto basin scale. The overall opinion on this issue seems to be in line with Reardon (2011) who cites Nicholas Fisher of Stony Brook University in New York: "after dilution, . . . , added radiation quickly becomes indistinguishable from the natural background level".

The aim of this study is to explore if this predication is confirmed by combining results of an oceanic general circulation model with a short review on the behavior of radioactive particles in marine environments. We focus on ^{137}Cs since the other major radionuclide released during the Fukushima accident, ^{131}I, has a short half-life of $\approx$ 8 days. ^{137}Cs, on the other hand, has a much longer half-life ($\approx$ 30 yr) and will remain in the marine environment long enough to participate in oceanic transport processes and other pelagic or sedimentary processes.

OSD
8, 1441–1466, 2011

We expect that, driven by concerns about radiation in seafood, a large dataset of radiation measurements in seawater will be collected and be available to the scientific community in the near future. Such a dataset could be a unique opportunity to benchmark the exchange, or interconnection, between the shelf sea and the open ocean as modeled with todays oceanic general circulation models. We feel that such a benchmark would be an important step towards a more comprehensive understanding of global biogeochemistry as expressed in models because the shelf seas host a significant fraction of oceanic primary production and carbon burial even though their surface area make up less than 10 % of the ocean's surface (e.g., Muller-Karger et al., 2005). Also, there is some evidence that large open-ocean regions are influenced by nutrients originating from the shelf or shelf break (e.g., Dietze et al., 2009). Taken together, the large share of production on the shelf, and the potential influence of shelf processes on the open ocean, imply that the interconnection (effected by the circulation) between the shelf and the open-ocean might well be an important – and according to e.g. Giraud et al. (2008) – a rather unquantified link in global carbon cycling.

Summing up, another aim of this study is to present a model estimate of exchange between the shelf and the open ocean off the coast of Japan which is to be evaluated when more measurements of radiation in seawater become available in the future.

In the following section we describe our main tool, the ocean general circulation model, and the numerical tracer release experiments. In Sect. 3 the circulation model is compared with observations. Section 4 presents results of the simulated tracers and provides a link to the general seasonal cycle of phytoplankton dynamics in the region. Section 5 puts our results into the context of what is known about the fate of ^{137}Cs in marine environments. Section 6 summarizes the main results.

OSD
8, 1441–1466, 2011

2 Method

2.1 Circulation model

We use the MOM4p0d (GFDL Modular Ocean Model v.4, Griffies et al., 2005) z-coordinate, free surface ocean general circulation model. The model region covers the entire global ocean with an enhanced meridional and zonal resolution around Japan. Figure 1a and b show the zonally and meridionally varying resolution. The vertical grid, with a total of 59 levels is shown in Fig. 1c. The bottom topography, shown in Fig. 1d, is interpolated from the ETOPO5 dataset, a 5 min gridded elevation data set from the National Geophysical Data Center (http://www.ngdc.noaa.gov/mgg/fliers/93mgg01.html). We use partial cells.

The atmospheric forcing consists of (6-hourly) wind stress, heat, and freshwater flux fields derived from the ERA-40 reanalyses from the European Centre for Medium-Range Weather Forecasts (ECMWF) (Uppala et al., 2005). In addition to the heat fluxes from the ECMWF, a flux correction restores sea surface temperatures (SSTs) with a time scale of 30 days to monthly mean SSTs derived from a blend of satellite products (Rathbone, 2006, personal communication). Sea surface salinity is restored to the World Ocean Atlas 2005 (Antonov et al., 2006) annual mean climatology with a timescale of 90 days. The vertical mixing of momentum and scalars is parameterized with the KPP approach of Large et al. (1994). The relevant parameters are (1) a critical bulk Richardson number of 0.3 and (2) a vertical background diffusivity and viscosity of $10^{-5}\,m^2\,s^{-1}$. We account for double-diffusive and nonlocal fluxes. The integration started from rest with initial temperatures and salinities interpolated from the World Ocean Atlas 2005 annual mean (Locarnini et al., 2006; Antonov et al., 2006) onto the model grid. After a spinup of 5 yr, covering the period 1993–1998, the model integrations presented in the following started in 1993. Note that 1993 is an arbitrary choice. Ideally, we would drive the circulation with actual, realistic fluxes. But even then, due uncertainties in the initial conditions and the highly non-linear dynamics of ocean eddies, it would be impossible to make an exact forecast. In all other respects,

OSD
8, 1441–1466, 2011

not described here, the model configuration is identical to the configuration without data assimilation described by Oke et al. (2005).

2.2 Tracer release

In order to simulate the accidental release of radioactive materials we embedded (online) an artificial tracer into the MOM4p0d circulation model. The tracer is released with a constant rate into one grid-box at 15 m depth next to the location of Fukushim-Daiichi, Japan. For technical reasons we did not use the surface box but one box below. Note that in our model, the difference between a surface and sub-surface release is negligible since the surface mixed layer is generally deeper than 20 m. The tracer is conservative, i.e. it does not decay but behaves like a dye, subject to mixing and advection only. On timescales much shorter than the half-life of ^{137}Cs the behavior of our artificial tracer mimics that of ^{137}Cs released directly into the sea off Fukushima-Daiichi.

There are, however a number of caveats: we do not take into account air-sea fluxes of radioactive particles since we do not have access to reliable deposition data. For the same reason, i.e. high uncertainty of the direct deposition to the sea, we use an artificial tracer and not an actual flux of ^{137}Cs. Hence, the results presented in this study are not directly comparable with measurements of radiation in seawater since our approach yields only relative concentrations – relative to the concentration modeled in the surface grid-box at the deposition site which covers an area of approximately 10 km × 10 km. More specifically, all relative concentrations shown in this study are referenced towards the temporal maximum concentration modeled in the surface grid-box at the deposition site. Note that other reference levels such as e.g. the concentration averaged in time over the release period result, due to the logarithmic scaling of results presented in this study, in negligible differences.

In order to account for uncertainties associated with the temporal evolution of the deposition of radiation and our inability to simulate an exact representation of the eddy-field we integrated an ensemble of 4 tracer releases (Table 1) all starting in model year 1993 after the 5-yr spinup of the circulation model. Table 1 lists the names of the

OSD
8, 1441–1466, 2011

ensemble members. The ensemble members CONFEB, CONMARCH, CONAPR differ with respect to when the tracer deposition was started. The release is not stopped but continuous throughout the integration. The idea behind this set of three is to explore if the tracer transport and dilution is a strong function of the initial state and evolution of the eddy field. Or, in other words, we seek for mutual patterns, unaffected by the uncertainties of the initial conditions and the rather chaotic behavior of eddy-dynamics. The ensemble member STOPMARCH is identical to CONMARCH except for the duration of the release which is not continuous but restricted to two months. The latter set of two explores the sensitivity of modeled concentrations with respect to the duration of the release.

3 Evaluation of the model circulation

One aim of this study is to explore the transport offshore, or fate, of a substance released into surface waters on the shelf off Japan. At least two preconditions, vital for a realistic simulation, have to be met: modeled mean surface currents and their variability must be realistic and, second, the surface mixed layer dynamics, which is the main process (on timescales considered here) mixing surface waters and dissolved substances to depth must also be realistic. Figure 2 shows that the main surface currents are represented by the model. Figure 3 shows that the variability associated with eddies, as expressed in variations of sea surface height, is comparable to observation from space in the eddy-resolving domain of the model. As for the surface mixed layer depth the situation is complicated by its extremely high variability both in space and time. This variability is, predominantly, a result of the strong eddy activity in the region: the formation and intensification of anti-cyclonic eddies is accompanied by downwelling fed by the convergence of horizontal surface currents which deepen the surface mixed layer. For cyclonic eddies, on the other hand, the reverse holds: formation and intensification comes along with a divergence of horizontal surface currents which pulls up the isopycnals and results in shallower surface mixed layers. Figure 4 compares

OSD
8, 1441–1466, 2011

a regional average of modeled surface mixed layers with data obtained from profiling Argo floats: given the high variability in both the model and the observations the model is consistent with the observations.

4 Simulated tracer distributions

In all simulations the tracer accumulates on the shelf between approximately 35.7° N and 38.25° N (upper panels of Fig. 5) with relative surface concentrations rarely exceeding 1/10 000 further offshore in the first 6 weeks. (Note that simulation STOPMARCH is not shown because it is identical to CONMARCH in the first two months and later in summer still very similar as Fig. 6 suggests.)

After 11 weeks following the start of the deposition the situation changes. Now, a large area offshore, within 140° E to 160° E and 32° N to 39° N, hosts surface concentrations exceeding 1/10 000 (lower panels of Fig. 5). The actual area with increased concentrations differs substantially among the model ensembles. These differences are not related to differences in the cross-shelf transport because the total amount of tracer on the shelf is identical to within less than 10 % among the ensemble members CONFEB, CONMARCH and CONAPR. The main mechanism causing the differences is the surface mixed layer dynamics: when the experiments start early in the year (CONFEB) the tracer is diluted over a deeper surface mixed layer relative to the later starts CONMARCH and CONAPR. Figure 6 highlights the strong correlation of offshore surface tracer concentration with surface mixed layer depth. Irrespective of the period of deposition (release only throughout March and May in experiment STOPMARCH and continuous release in CONMARCH) maximum concentrations appear in late May after the surface mixed layer, on average, has shallowed to values less than 50 m. Then, later in autumn and winter, concentrations decrease rapidly as sea-air heat-fluxes destabilize the water column down to more than 200 m.

An intercomparison of modeled tracer distribution with climatological surface chlorophyll concentrations observed from space (calculated from SeaWiFS level 3 mapped

OSD
8, 1441–1466, 2011

8-day composites from http://seadas.gsfc.nasa.gov) links our abiotic simulations to biotic productivity in the region (Fig. 7): in April when the regional spring bloom has not yet started offshore (due to unfavorable light conditions determined by a combination of deep surface mixed layer depth and rather low solar radiation entering the ocean, although Behrenfeld (2010) raises doubt on this issue), enhanced tracer concentrations (i.e. exceeding 1/10 000) at the surface are restricted to the shelf. In May, enhanced tracer concentrations meet an already decaying, northwards receding, spring-bloom offshore. In June, enhanced concentrations reside in a post bloom environment where most of the organic material, built up during the bloom, has already been consumed by higher trophic levels, and/or been exported to depth.

The timing of enhanced tracer concentrations offshore in combination with the typical evolution of the regional spring-bloom on one hand and the high accumulation of radiation in marine biota (via absorption or incorporation) on the other hand poses, indeed, the question if "... bioaccumulation could be a boon ... in terms of cleaning up the ocean" (Reardon, 2011).

5 Discussion

Results presented so far indicate that concentrations of ^{137}Cs offshore, may well exceed 1/10 000 relative to *average* concentrations in an area of 10 km × 10 km at the deposition site. Based on the sparse measurements available to us at this time, we can not transfer this model estimate into actual ^{137}Cs concentrations. Further uncertainties arise from coastal processes: there are the small-scale processes below the mesoscale which are not resolved by our circulation model. And, the question remains, to what extend ^{137}Cs can be considered as a conservative, or inertial, tracer (similar to a simple dye) because additional complexity comes into play through processes such as adsorption, desorption, bioaccumulation, sedimentation, re-suspension, bioturbation and diagenesis (Kobayashi et al., 2007). It is straightforward to assume that the effect of these processes (dubbed particle reactivity) is stronger in the coastal zone

OSD
8, 1441–1466, 2011

on the shelf, where water depths are shallow, chlorophyll concentrations and associated biomass are rather high, and air-sea fluxes of particles, or dust, originating from land are also higher than further offshore. The latter point is mirrored by published, apparently contradictory, approaches to model oceanic ^{137}Cs: Kobayashi et al. (2007) conclude, based on simulations of ^{137}Cs released off Sellafield into the rather shallow and productive Irish Sea that "... the removal of radionuclides by particles is an important factor for the calculation of the particulate radionuclides migration".

Likewise, Periáñez and Elliott (2002) included a parameterization of particle reactivity in their simulation of ^{137}Cs in the English Channel. In contrast, Tsumune et al. (2011) who simulate ^{137}Cs in the world's ocean start their introduction with the bold statement: "Oceanic ^{137}Cs is an inertial tracer that behaves according to physical processes in the ocean without any biogeochemical interaction".

As far as we can see, a comprehensive understanding of the fate of ^{137}Cs in a marine environment, where vertical fluxes of organic and inorganic particles might drive associated ^{137}Cs fluxes due to uptake or adsorption, has not been achieved yet. This might also apply to the open ocean where Tsumune et al. (2011), based on the assumption that ^{137}Cs is "inertial", model a strong underestimation of ^{137}Cs at depth ($>\approx 500$ m), in general. Although Tsumune et al. (2011) argue that their misfit is caused by a deficient eddy-parameterization it can not be ruled out that neglected vertical fluxes, other than those associated to the circulation, contribute to their misfit.

What remains is to sum up observational studies. Most information comes from studies in the Baltic Sea carried out in the aftermath of the Chernobyl accident. This is unfortunate since this brackish, mediterranean, highly productive and shallow (average depth is 50 m) sea is hardly comparable to neither the coastal nor the open Pacific Ocean. Then again, it outlines major uncertainties hindering the assessment of the long or mid-term effects of the Fukushima accident on the marine environment.

OSD
8, 1441–1466, 2011

5.1 Baltic Sea

The deposition of ^{137}Cs after the Chernobyl accident on 26 April 1986 from the air to the Baltic Sea showed a strong spatial variability. The highest activities in 1986 were measured in the Bothnian Sea and the Gulf of Finland (HELCOM, 1995; Ilus, 2007). The measured concentration peaked in the first half of May at 5200 Bq m^{-3} and decreased quickly thereafter (Ilus, 2007). This suggests a strong impact of mixing and advection in this semi-enclosed basin. In the years following the accident, concentrations in seawater remained relatively high, up 600 Bq m^{-3} in the Bothnian Sea and Gulf of Finland, followed by a sudden decline. Recent concentrations exhibit a quite homogeneous spatial distribution (HELCOM, 2009). In 2006, 20 years after the Chernobyl accident only 18.5 % (870 TBq) of the total load entering the Baltic (4700 TBq) could still be found in the water column ((HELCOM, 2009)). Adsorption of radionuclides onto particles may have played a role in transferring the surface signal to the sediment, where ^{137}Cs slowly accumulated: in 1989–1990, sinking matter in the Gulf of Finland showed about the same concentrations of ^{137}Cs as the sediment (HELCOM, 1995), suggesting a tight coupling between surface and sediment. Ilus (2007) notes that "The sinking rate of the fallout nuclides was relatively high owing to the coincidence of the end phase of the phytoplankton spring maximum, when the radionuclides were transported downwards by the dead plankton algae."

As a consequence, sediment radiocesium concentrations reflect to a large extent the post-Chernobyl concentrations in the surface seawater (HELCOM, 1995), especially on longer time scales (HELCOM, 2009). While in 1990–1991 only about 26–30 % of the Chernobyl input to the Baltic Sea was located in the sediment, the fraction increased up to > 50 % (2400 TBq) in 2006. Much of the accumulation took place in the Bothnian Sea and in the Gulf of Finland (HELCOM, 2009; Ikäheimonen et al., 2009).

The pattern of deposition and seawater concentration after the accident was also reflected in the distribution in biota, where the Cs isotopes were the dominating artificial radionuclide. The biota responded quickly to increased levels of ^{137}Cs (HELCOM,

OSD
8, 1441–1466, 2011

1995, 2009). The initial peak was followed by a gradual decline of activities in e.g. in herring, flat fish, or sea weed (HELCOM, 2009). Despite the relatively high concentrations in the organisms, Ikäheimonen et al. (2009) omitted the biota from their budget calculations, because the "importance of the biota in removing or binding ^{137}Cs [...] is so low (< 1 %)". On the other hand they highlighted the importance of (sediment) particles and organic matter for binding radionuclides.

Summarizing, the emerging picture is one where on timescales of months to years (following the deposition) transport processes such as advection and mixing are dominating. On longer timescales (years to decades) the sediment and associated processes become important. This is also reflected in the different effective half-lives (i.e. half-lives that comprise physical, biological, and chemical processes) of ^{137}Cs in the Bothnian Sea, being 2.5 yr in the period 1986–1988, and 9 yr in the period 1993–2006 (HELCOM, 2009). The explicit role of small pelagic organisms and particles, however, remains unclear in these studies.

5.2 Laboratory studies

Little is known about the dynamics of ^{137}Cs in the lower trophic levels of the pelagic food chain. IAEA (2004) suggests volumetric concentration factors (activity in organism divided by activity in ambient seawater) of 20 for marine phytoplankton, based on the work by Heldal et al. (2001). A closer look at Heldal et al. (2001) reveals that the situation is complex: their observations show concentration factors between 0–60 for five different, actively growing phytoplankton species. However, when incubated in the dark, concentration factors were enhanced for many species. In the case of the diatom *Thalassiosira pseudonana* they increased up to values of 200 after 6 days.

While the relatively low uptake of ^{137}Cs of actively growing algae may be attributed to the high potassium levels in seawater, which prevent the uptake of the comparatively low Cs concentrations (Heldal et al., 2001), the larger concentration factors of non-growing (probably senescent) phytoplankton could potentially be attributed to mucus or organic substances adhering to the cells wall or diatom frustules, which may

OSD
8, 1441–1466, 2011

facilitate adsorption of the metal ions to the cell surface. This process has also been hypothesized to be of importance for the high ^{137}Cs concentrations of benthic diatoms in the Bothnian Bay (Snoeijs and Notter, 1993). The importance of dead phytoplankton for the transfer of ^{137}Cs to the sediment has also been noted by Ilus (2007).

There is evidence that ^{137}Cs concentration factors increase along the food chain. IAEA (2004) suggests a concentration factor of 40 for marine zooplankton, 50–60 for crustaceans and molluscs and 100 for fish. In a laboratory experiment using the lighter isotope ^{134}Cs Mathews and Fisher (2008) found a concentration factor of 130 in marine prymnesiophyte *Isochrysis galbana* which they grew to feed animals. (Note that Heldal et al. (2001) and IAEA (2004) estimated lower values for the heavier isotope ^{137}Cs.) After feeding animals with these labeled algae, Mathews and Fisher (2008) found a high retention of this metal for brine shrimp (*Artemia salina*), sea bream (*Sparus auratus*) and sea bass (*Dicentrarchus labrax*).

5.3 A rough estimate of the impact of biota and particle scavenging in the area of interest

A rough scaling based on the concentration factors of ^{137}Cs in phytoplankton (reviewed in Sect. 5.2) and the chlorophyll concentrations off Japan (Fig. 7) suggests that the impact of biota on surface concentrations of ^{137}Cs is small: assuming a chl-*a* concentration around 1 mg m^{-3} and a cell size of 10 µm yields a cell density of $\approx 7 \times 10^5$ cells per liter (using the chlorophyll-to-volume relationship given by Montagnes et al., 1994). This cell density converts to a phytoplankton-volume per volume-seawater ratio of $\approx 0.4 \times 10^{-6}$, or 0.4 ppm. Imposing a relatively high (i.e. closer to the values suggested by Mathews and Fisher (2008) than to the values given by Heldal et al. (2001)) concentration factor of 100 results in a ^{137}Cs activity bound by phytoplankton that is far less than 1 % of that of ambient seawater. In other words, the integrated activity in phytoplankton is low compared to that integrated over the water parcel hosting the phytoplankton because phytoplankton cells comprise only a tiny fraction of the total volume of a water parcel. This does also hold for 1.) chl-*a* concentrations an order

OSD
8, 1441–1466, 2011

of magnitude larger which may be found in April–June on the coastal shelf off Japan (Fig. 7a–c) and 2.) for the receding and probably senescent bloom further offshore (Fig. 7c), even though, in the latter case, work by Heldal et al. (2001) suggests higher concentration factors of 200 (for aged or dead diatoms) and, further, additional increases along the food chain might come into play (IAEA, 2004; Mathews and Fisher, 2008).

Now, in order to assess the flux of ^{137}Cs from the surface to depth via vertical export of biomass an assumption on the vertical flux of particulate organic material has to be made. In the following we consider a hypothetical and unrealistically extreme case to derive an upper bound: assuming a phytoplankton bloom which grows up to 10 mg chl-*a* m^{-3} every day and is exported to depth every night yields, in combination with a concentration factor of 200, a removal or "cleansing" rate of 4 ppm $\times 200 = 8 \times 10^{-4}$ per day. This means that 0.08 % of the ^{137}Cs in seawater at the surface is exported to depth every day and, even if the conditions described above would persist over a whole year, about 75 % of any initial radionuclide pulse would remain in the water column.

Note that this low estimate of biotically driven vertical ^{137}Cs flux (which is solely based on the pelagic autotrophic community and concentrations factors measured in the laboratory) is apparently inconsistent with the tight pelagic-benthic coupling observed in the Baltic Sea (Ilus, 2007; HELCOM, 2009; Ikäheimonen et al., 2009), the Irish Sea (Kobayashi et al., 2007), and the English Channel (Periáñez and Elliott, 2002). It seems straightforward to resolve this apparent inconsistency by arguing that the tight pelagic-benthic coupling in the examples above is driven by a combination of high, probably abiotic, particle loads and shallow water depths. This is in line with high ^{134}Cs adsorption rates of sediment particles (0.18 cm d^{-1}) measured by Nyffeler et al. (1984) according to Periáñez (1998). (Note that we failed to retrace how Periáñez (1998) converted the reaction rate constant estimates of Nyffeler et al. (1984) to exchange velocities or adsorption rates.) The caveat that remains, however, is that Nyffeler et al. (1984) report similar (i.e. in the same order of magnitude) estimates for material collected from sediment traps. Hence they might be applicable to live or senescent phytoplankton cells

OSD
8, 1441–1466, 2011

(as was assumed in an open ocean modeling study by Periáñez, 1998) and this would change the above estimate based on concentration factors derived from incubations drastically: again, we consider the above example of a hypothetical unrealistic phytoplankton bloom growing up to 10 mg Chl m^{-3} each day and being exported to depth each night. Assuming a cell size of 10 µm yields a total cell surface area of about 2.4 m^2 per m^3 seawater. Using the adsorption rate of (Nyffeler et al., 1984) implies that only ≈ 20 % of any initial radionuclide pulse remains in the water column after one year. Choosing a chlorophyll value of 1 mg Chl m^{-3} which is more representative for the situation offshore implies that 85 % remains in the water column after one year.

We conclude, based on a hypothetical unrealistically extreme bloom dynamic (or export production) that on timescales of months the removal of ^{137}Cs by marine biota from the surface is a minor process offshore. This assessment is backed by the fact that the above calculations do not take into account desorption from the particles, which may further decrease the "cleansing" effect of marine biota. For longer timescales and coastal environments, however, there is evidence that vertical (biotic and abiotic) particle transport drives a considerable associated transport of ^{137}Cs from the surface to depth.

6 Conclusions

We set out to explore the fate of ^{137}Cs released directly from the land to the ocean at Fukushima-Daiichi, Japan based on an artificial tracer (similar to a simple dye) released in an oceanic general circulation model. Our approach is problematic for a number of reasons, including uncertainties in the magnitude and the temporal evolution of the release, and our incapability to simulate the chaotic behavior of eddy dynamics on a one-to-one basis. However, by exploring a suite of model integrations and focussing on concentrations relative to an areal average (covering ≈ 100 km^2) at the release site, a number of consistent results emerge: In all simulations, *relative* concentrations exceeding 1/10 000 meet a receding or senescent spring bloom offshore. The size of this

OSD
8, 1441–1466, 2011

area is strongly determined by surface mixed layer dynamics which is well reproduced by the model. Further, we find that the cross-shelf transport is surprisingly insensitive towards changes of the initial conditions of the eddy-field since all our model estimates agree within 10 %.

A review on the question to what extent ^{137}Cs can be considered as an "inertial" tracer (i.e. unaffected by particle reactivity) combined with a rough calculation, implies that the interaction between pelagic biota and ^{137}Cs (which we neglected in our numerical experiments) does not drive a significant vertical flux offshore on the timescales considered here. This is in contrast to Reardon (2011) who speculates that "... bioaccumulation could be a boon ... in terms of cleaning up the ocean". However, on longer timescales, or if processes like sediment burial and resuspension or uptake by the benthic biota come into play, the assumption of ^{137}Cs as an "inertial" tracer might well be fundamentally wrong.

We conclude that a comprehensive set of ^{137}Cs measurements off Fukushima-Daiichi, Japan could help to answer a number of questions: first they can be used to assess the interconnection between the shelf and the open ocean as modeled with state-of-the-art oceanic general circulation models. Further, they can help to constrain the uncertainty associated with particle reactivity of ^{137}Cs. It is noteworthy that research on the latter point will also make ^{137}Cs more suitable as a benchmark for global circulation models as is the case to-date.

Acknowledgements. Discussions with Claus Böning, Andreas Oschlies and Ignacio Pisso are appreciated. Thanks also to the GFDL modeling community for advancing and distributing MOM. It is a splendid research platform. The model integrations were performed on a NEC-SX9 at the University Kiel. We used WOA 2005 from NOAA, converted by Mark Collier at CSIRO. This study uses Argo data that "were collected and made freely available by the International Argo Program and the national programs that contribute to it (http://www.argo.ucsd.edu, http://argo.jcommops.org). The Argo Program is part of the Global Ocean Observing System."

OSD
8, 1441–1466, 2011

References

Antonov, J. I., Locarnini, R. A., Boyer, T. P., Mishonov, A. V., and Garcia H. E.: World Ocean Atlas 2005, vol. 2, edited by: Levitus, S., NOAA Atlas NESDIS 62, US Government Printing Office, Washington, D.C., 182 pp., 2006. 1444

Behrenfeld, M. J.: Abandoning Sverdrup's critical depth hypothesis on phytoplankton blooms, Ecology, 4, 97–9897, 2010. 1448

Dietze, H., Matear, R. J., and Moore, T. S.: Nutrient supply to anticyclonic meso-scale eddies off Western Australia estimated with artificial tracers released in a circulation model, Deep-Sea Res. Pt. I, 56, 9, 1440–1448, doi:10.1016/j.dsr.2009.04.012, 2009. 1443

Giraud, X., Le Qéré, C., and da Cunha, L. C.: Importance of coastal nutrient supply for global ocean biogeochemistry, Global Biogeochem. Cy., 20, 2, doi: 10.1029/2006GB002717, 2008. 1443

Griffies, S., Gnanadesikan, A., Dixon, K., Dunne, J., Gerdes, R., Harrison, M., Rosati, A., Russell, J., Samuels, B., Spelman, M., Winton, M., and Zhang, R.: Formulation of an ocean model for global climate simulations, Ocean Sci., 1, 45–79, 2005, http://www.ocean-sci.net/1/45/2005/. 1444

HELCOM: Radioactivity in the Baltic Sea, 1984–1991, Baltic Marine Environment Protection Commission – Helsinki Commission, Balt. Sea Environ. Proc. No. 61, Helsinki, 175 pp., 1995. 1450

HELCOM: Radioactivity in the Baltic Sea, 1999–2006, Baltic Marine Environment Protection Commission – Helsinki Commission, Balt. Sea Environ. Proc. No. 117, Helsinki, 60 pp., 2009. 1450, 1451, 1453

Heldal, H. E., Stupakoff, I., and Fisher, N. S.: Bioaccumulation of ^{137}Cs and ^{57}Co by five marine phytoplankton species, J. Environ. Radioactiv., 57, 231–236, 2001. 1451, 1452, 1453

IAEA: Sediment distribution coefficients and concentration factors for biota in the marine environment, International Atomic Energy Agency, Technical Reports Series, 422, Wien, 95 pp., 2004. 1451, 1452, 1453

Ilus, E.: The Chernobyl accident and the Baltic Sea, Boreal Environ. Res., 12, 1–10, 2007. 1450, 1452, 1453

Ikäheimonen, T. K., Outola, I., Vartti, V.-P., and Kotilainen, P.: Radioactivity in the Baltic Sea: inventories and temporal trends of ^{137}Cs and ^{90}Sr in water and sediments, J. Radioanal. Nucl. Ch., 282, 419–425, doi:10.1007/s10967-009-0144-1, 2009. 1450, 1451, 1453

OSD
8, 1441–1466, 2011

Kobayashi, T., Otosaka, S., Togawa, O., and Hayashi, K.: Development of a non-conservative radionuclides dispersion model in the ocean and its application to surface Cesium-137 dispersion in the Irish Sea, J. Nucl. Sci. Technol., 44 (2), 238–247, 2007. 1448, 1449, 1453

Locarnini, R. A., Mishonov, A. V., Antonov, J. I., Boyer, T. P., and Garcia, H. E.: World Ocean Atlas 2005, vol. 1: Temperature, edited by: Levitus, S., NOAA Atlas NESDIS 61, US Government Printing Office, Washington, D.C., 182 pp., 2006. 1444

Large, W. G., McWilliams, J. C., and Doney S. C.: Oceanic vertical mixing – a review and a model with a nonlocal boundary-layer parameterization, Rev. Geophys., 32 (3), 363–403, 1994. 1444

Mathews, T. and Fisher, N. S.: Trophic transfer of seven trace metals in a four-step marine food chain, Mar. Ecol.-Progr. Ser., 367, 23–33, doi:10.3354/meps07536, 2008. 1452, 1453

Montagnes, D. J. S., Berges, J. A., Harrison, P. J., and Taylor, F. J. R.: Estimating carbon, nitrogen, protein, and chlorophyll *a* from volume in marine phytoplankton, Limnol. Oceanogr., 39 (5), 1044–1060, 1994. 1452

Muller-Karger, D. F., Varela, R., Thunell, R., Luerssen, R., Hu, C., and Walsh, J. J.: The importance of continental margins in the global carbon cycle, Geophys. Res. Lett., 32, L01602, doi:10.1029/2004GL021346, 2005. 1443

Nyffeler, U. P., Li, Y.-H., and Santschi, P. H.: A kinetic approach to describe trace-element distribution between particles and solution in natural aquatic systems, Geochim. Cosmochim. Ac., 48, 1513–1522, 1984. 1453, 1454

Oke, P. R., Schiller, A., Griffin, D. A., and Brassington, G. B.: Ensemble data assimilation for an eddy-resolving ocean model of the Australian region, Q. J. Roy. Meteor. Soc. 131, 3301–3311, 2005. 1445

Periáñez, R.: Modelling the distribution of radionuclides in deep ocean water columns. Application to ^{3}H, ^{137}Cs and ^{239,240}Pu, J. Environ. Radioactiv., 38, 173–194, 1998. 1453, 1454

Periáñez, R. and Elliott, A. J.: A particle-tracking method for simulating the dispersion of non-conservative radionuclides in coastal waters, J. Environ. Radioactiv., 58, 13–33, 2002. 1449, 1453

Reardon, S.: Fukushima radiation creates unique test of marine life's hardiness, Science, 332, 292–292, 2011. 1442, 1448, 1455

Snoeijs, P. and Notter, M.: Benthic diatoms as monitoring organisms for radionuclides in a brackish-water coastal environment, J. Environ. Radioactiv., 18, 23–52, 1993.

OSD
8, 1441–1466, 2011

Tsumune, D., Aoyama, M., and Hirose, K.: Behavior of ^{137}Cs in the North Pacific in an ocean general circulation model, J. Geophys. Res., 108 (C8), 3262, doi:10.1029/2002JC001434, 2003. 1452

Tsumune, D., Aoyama, M., Hirose, K., Bryan, F. O., Lindsay, K., and Danabasoglu, G.: Transport of ^{137}Cs to the Southern Hemisphere in an ocean general circulation model, Prog. Oceanogr., 89, 38–48, doi:10.1016/j.pocean.2010.12.006, 2011.

Uppala, S., Kallberg, P., Simmons, A., Andrae, U., da Costa Bechtold, V., Fiorino, M., Gibson, J., Haseler, J., Hernandez, A., Kelly, G., Li, X., Onogi, K., Saarinen, S., Sokka, N., Allan, R., Andersson, E., Arpe, K., Balmaseda, M., Beljaars, A., van de Berg, L., Bidlot, J., Bormann, N., Caires, S., Chevallier, F., Dethof, A., Dragosavac, M., Fisher, M., Fuentes, M., Hagemann, S., Holm, E., Hoskins, B., Isaksen, L., Janssen, P., Jenne, R., McNally, A., Mahfouf, J.-F., Morcrette, J.-J., Rayner, N., Saunders, R., Simon, P., Sterl, A., Trenberth, K., Untch, A., Vasiljevic, D., Viterbo, P., and Woollen, J.: The ERA-40 re-analysis, Q. J. Roy. Meteor. Soc., 131, 2961–3012, 2005. 1449

1444

OSD

8, 1441–1466, 2011

Table 1. List of model integrations.

Short name	Description
CONFEB	continuous tracer release, starting on 1 Feb
CONMARCH	continuous tracer release, starting on 1 Mar
CONAPR	continuous tracer release, starting on 1 Apr
STOPMARCH	tracer release is restricted to the period 1 Mar to 30 Apr

OSD
8, 1441–1466, 2011

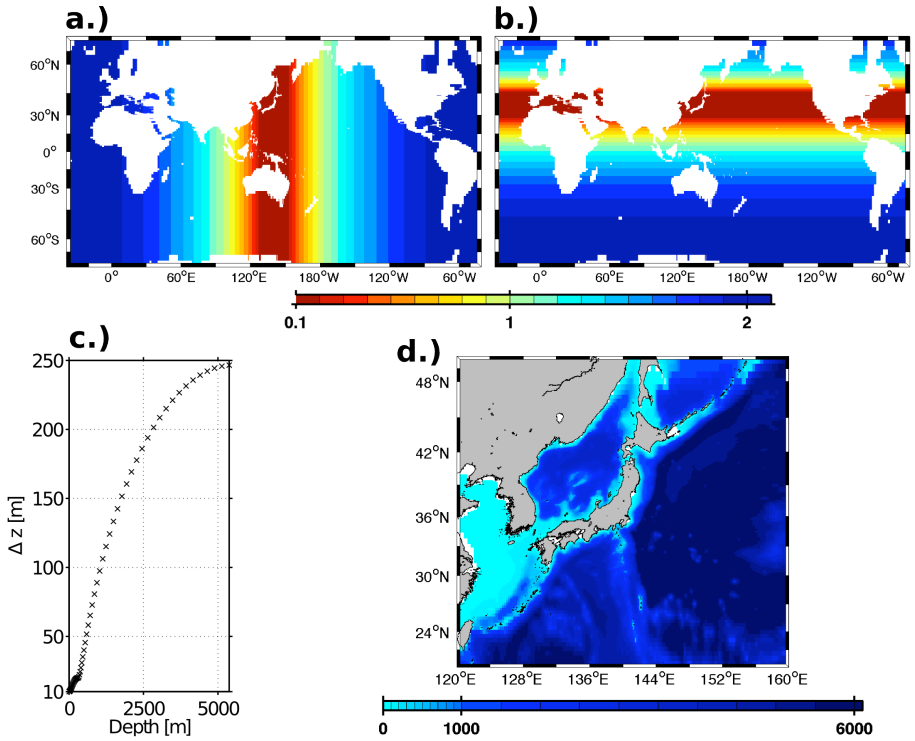

Fig. 1. The model grid. Panel (**a** and **b**) are horizontal and meridional resolution in units degrees. Panel **(c)** shows the vertical resolution Δz as a function of depth in units meters. Panel **(d)** shows the model bathymetry (in units meter) in the region of interest. (White areas are considered as land by the model while the gray patches outline the actual land distribution.)

OSD
8, 1441–1466, 2011

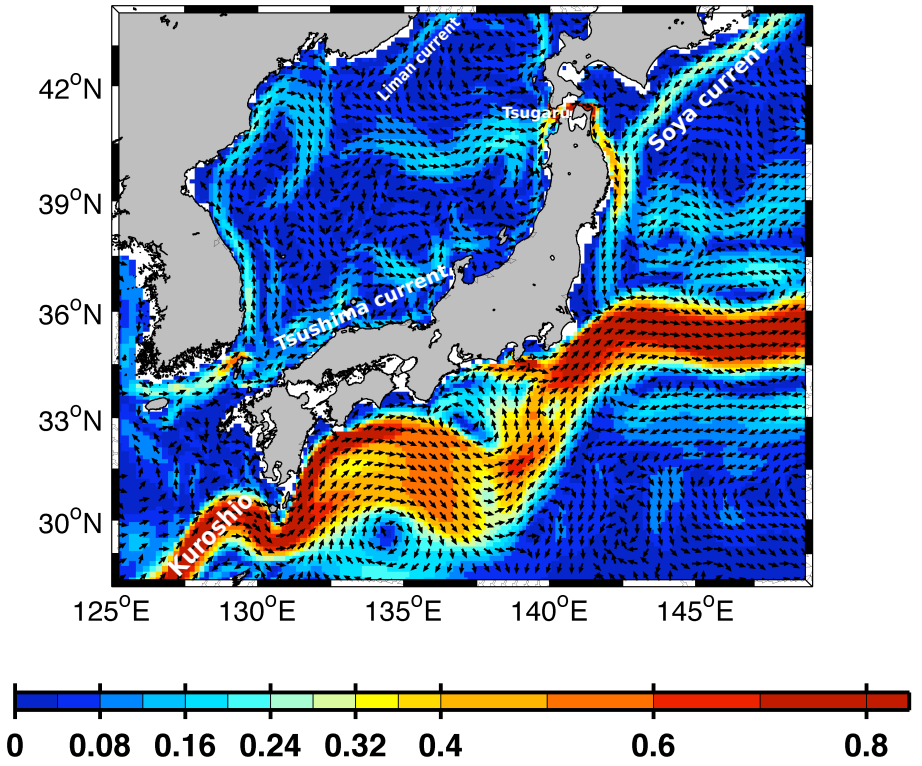

Fig. 2. Modeled surface currents, 3-yr average. The color shading denotes absolute velocity in units $m\,s^{-1}$. The arrows indicate the direction of the currents. Note that the actual model resolution is three times higher (in both meridional and zonal direction) than indicated by the arrows.

OSD
8, 1441–1466, 2011

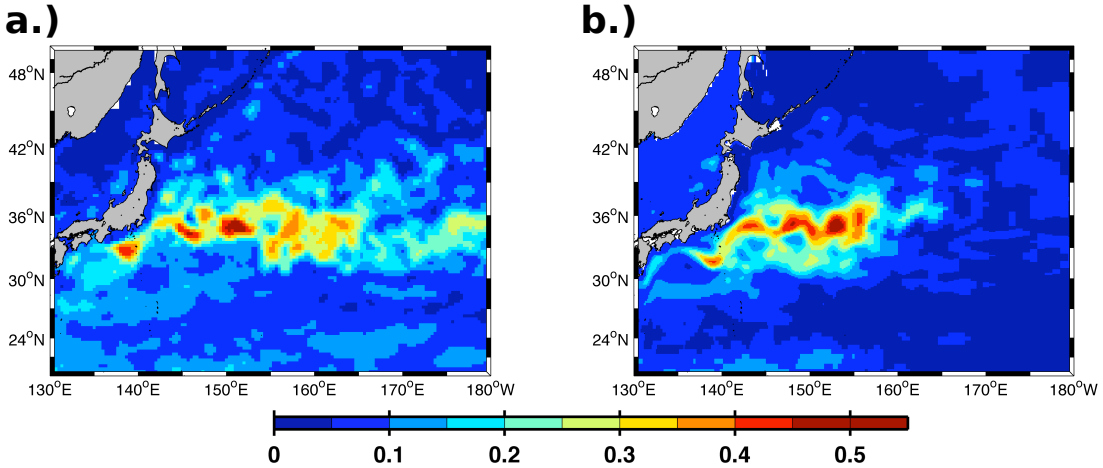

Fig. 3. Sea surface height variability (standard deviation) in units meters. Panel **(a)** is calculated from weekly, gridded, satellite observations from 1993. Panel **(b)** is based on weekly snapshots of the model year 1993.

OSD
8, 1441–1466, 2011

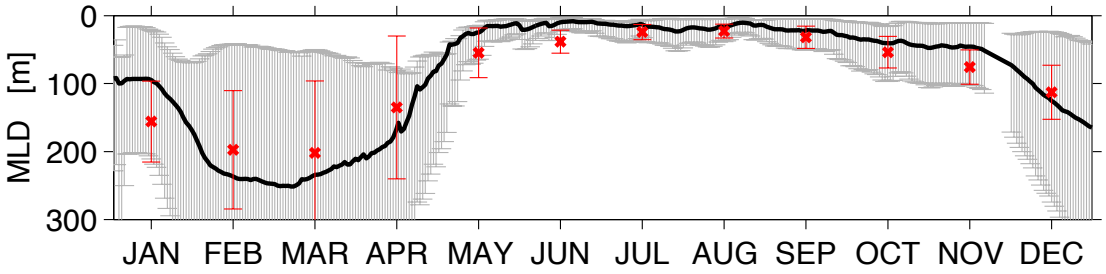

Fig. 4. Surface mixed layer depth (defined as the depth where density σ_0 exceeds surface values by 0.125) averaged over the region bounded by 130° E to 160° E and 33° N to 42° N (grey dashed line in Fig. 7). The black line is calculated from modeled, daily snapshots of model year 1993. The gap in November is caused by files corrupted during integration. The vertical grey lines denote the standard deviation which represents the modeled spacial variability at a given day. The red crosses are calculated from a total of 1796 Argo profiles in the period 1998 to 2004. The vertical red line is the standard deviation calculated from all observations found in the region at a given month.

OSD
8, 1441–1466, 2011

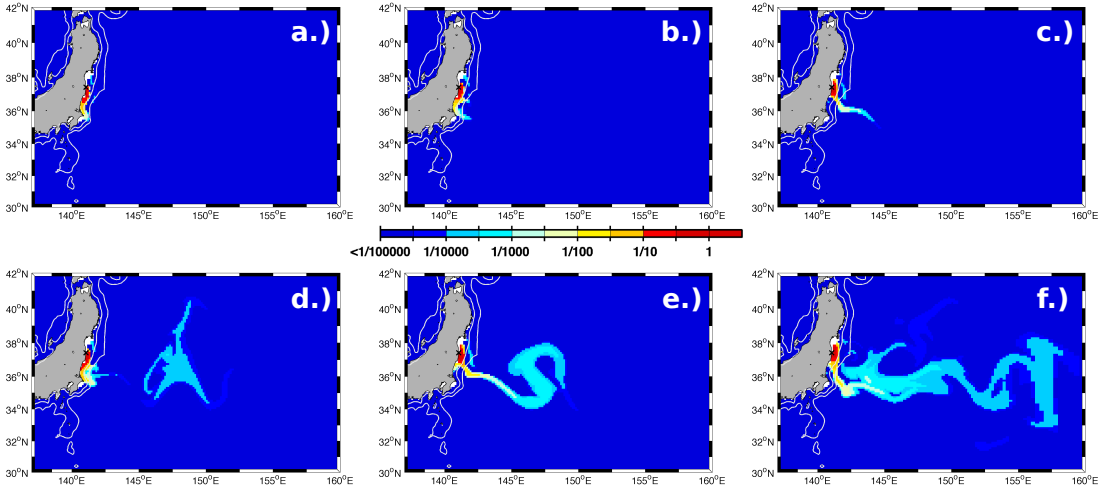

Fig. 5. Modeled ensemble of relative tracer concentrations integrated with continuous tracer release. Upper (lower) panels after 6 (11) weeks of release. The panels (**a** and **d**) refer to simulation CONFEB, panels (**b** and **e**) to simulation CONMARCH and the panels (**c** and **f**) to simulation CONAPR (see Table 1 for naming convention). The white contours denote the 200 m and 1000 m isobath.

OSD
8, 1441–1466, 2011

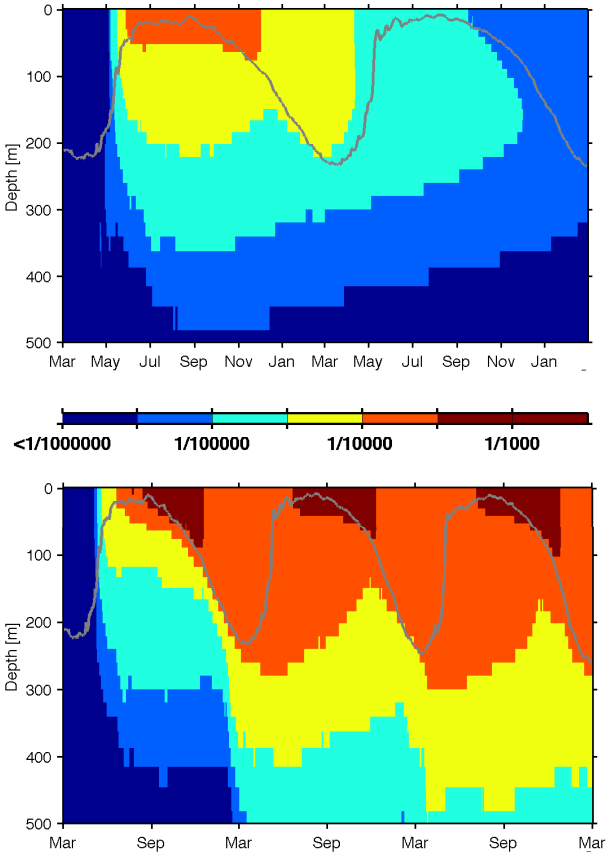

Fig. 6. Horizontal average (130° E to 160° E and 33° N to 42° N, see Fig. 7) of relative tracer concentrations. The grey thick line denotes the temporal evolution of the surface mixed layer depth. The upper (lower) panel refers to ensemble member STOPMARCH (CONMARCH).

OSD
8, 1441–1466, 2011

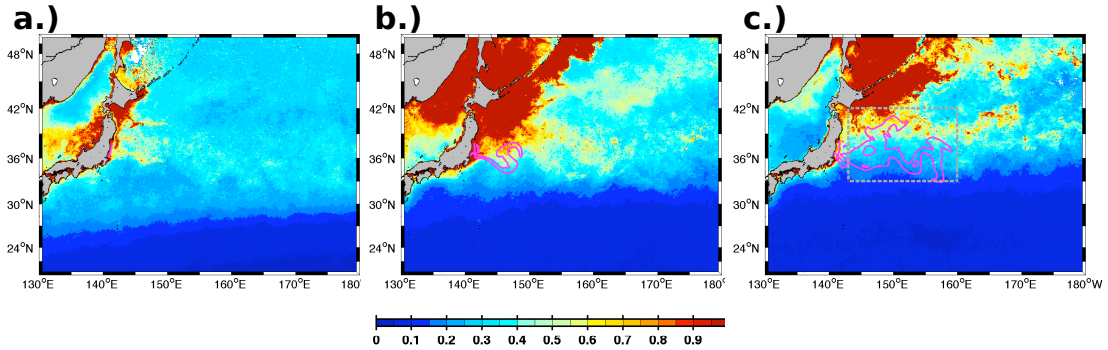

Fig. 7. Observed chlorophyll and modeled, relative tracer concentrations in April, May and June **(a–c)**, respectively). The colored shading denotes climatological chlorophyll concentrations observed from space in mg chl-*a* m^{-3}. The magenta contour refers to that region where modeled concentrations exceed 1/10 000 relative to the temporal maximum found at the release site. The grey dashed box in panel **(c)** (130° E to 160° E and 33° N to 42° N) denotes the region which is explored in Figs. 6 and 4.

OSD
8, 1441–1466, 2011